9th Asia-Pacific Conference on Wind Engineering
Auckland, New Zealand
3-7 December 2017

Numerical Method for Buffeting Simulation of Cable-Supported Bridges in Time-Domain

R. Soltys[1], M. Tomko[1] and S. Kmet[1]

[1]Institute of Structural Engineering,
Faculty of Civil Engineering, Technical University of Kosice, Kosice, 042 00, Slovak Republic

Abstract

A buffeting response simulation method of bridges in time domain is proposed in the paper. As an example, the buffeting response of a cable-stayed footbridge has been computed. The method consists of a computational structural dynamics (CSD) model coupled with a computational fluid dynamics (CFD) model, involving artificial boundary-layer turbulent inflow. The fluctuating spatially-correlated wind velocities are generated using the Shinozuka–Deodatis method with applied wind characteristics computed from in-situ measurements. The CFD model is represented by a solution of Navier–Stokes equations for incompressible fluid flow in two-dimensional planes located perpendicularly to the longitudinal axis of the bridge deck. 2D planes along the deck are applied in order to reduce high computational demands, which are more significant the longer the structure is. The equation of motion is solved using the finite element method in the CSD model. The coupling of the CSD and CFD models is realized via fluid-structure interface (FSI) adopted in ADINA commercial code.

Introduction

Wind-induced response is complex due to the interaction between the flexible structure and wind. There are several known types of wind-induced response for bridge decks, such as vortex-induced vibrations (VIVs), flutter, buffeting and galloping, which are dependent on wind velocity. At specific wind velocities aerodynamic response interaction may occur, e.g. buffeting with VIVs usually investigated on physical models and buffeting with flutter usually investigated on mathematical models. The oncoming turbulent wind may induce a buffeting response of structures, while the VIVs predominantly occur under constant flow velocity. Both, the buffeting and the VIVs may cause fatigue damage of slender structures and bridges. Buffeting response prediction of bridges was proposed by A.G. Davenport [5] in a frequency domain based on quasi-steady theory. Later developed methods include multi-mode behaviour [10], aerodynamic coupling [13], and probability-based approach using Monte Carlo simulation [7]. A time domain approach for the buffeting analysis of a bridge deck were presented in [1,12]. The probabilistic nature of wind turbulence and aeroelastic characteristics to single-mode buffeting was analyzed in [4]. In order to carefully consider the dynamic action of gusty wind acting on the bridge the wind turbulence characteristics were estimated from in-situ wind velocity measurements [9]. Nowadays, CFD is widely used through various wind engineering problems, including bridge aerodynamics [3]. Coupled CFD with CSD methods were applied in [8,11,14].

In this paper the numerical buffeting response simulation method acting in a time domain is presented. The proposed method is demonstrated on a cable-stayed footbridge, as an example. The wind induced response involves aeroelastic behaviour of the deck and aerodynamic excitation of the cables and the pylon. The random nature of turbulent wind is represented by wind time-histories applied in the numerical model.

Structural Model

The CSD model is described by an equation of motion in matrix form

$$\boldsymbol{M}\ddot{\boldsymbol{U}} + \boldsymbol{C}\dot{\boldsymbol{U}} + \boldsymbol{K}\boldsymbol{U} = \boldsymbol{R} + \boldsymbol{F}_S \qquad (1)$$

where $\boldsymbol{M}$, $\boldsymbol{C}$ and $\boldsymbol{K}$ are the matrices of mass, damping, and tangencial stiffness, respectively. $\ddot{\boldsymbol{U}}$ denotes the nodal acceleration vector, $\dot{\boldsymbol{U}}$ and $\boldsymbol{U}$ are the velocity and displacement nodal vectors. Damping matrix in equation (1) is expressed in the form of proportional damping

$$\boldsymbol{C} = \alpha\boldsymbol{M} + \beta\boldsymbol{K} \qquad (2)$$

where α and β are the Rayleigh coefficients. The finite element method is applied to discretize the CSD model in space and the Newmark time integration method is applied to solve the equation of motion for each time step. The geometrical nonlinearity is involved via a tangential stiffness matrix which require iterative and Newton–Raphson procedures. $\boldsymbol{R}$ is the applied aerodynamic loading vector and $\boldsymbol{F_S}$ is the nodal force vector applied from fluid flow stress along the fluid-structure interface.

Fluid Model

The CFD model around the structure is described by the Navier–Stokes equations expressed in the conservative forms for mass, momentums and energy, respectively [2]

$$\frac{\partial \rho}{\partial t} + \nabla \bullet (\rho \boldsymbol{v}) = 0, \qquad (3)$$

$$\frac{\partial \rho \boldsymbol{v}}{\partial t} + \nabla \bullet \left(\rho \boldsymbol{v}\boldsymbol{v}^T - \tau\right) = \boldsymbol{F}_S \qquad (4)$$

$$\frac{\partial \rho E}{\partial t} + \nabla \bullet \left(\rho \boldsymbol{v} E - \tau \bullet \boldsymbol{v} + \boldsymbol{q}\right) = \boldsymbol{F}_S \bullet \boldsymbol{v} + q_S, \qquad (5)$$

where t is time, ρ is the fluid density, $\boldsymbol{v}$ is the velocity vector, τ is the stress tensor, E is the specific total energy, q is the heat flux and q_S is the specific rate of heat generation. The CSD model coupled with CFD model are applied in order to compute aeroelastic forces $\boldsymbol{F_S}$ acting on the structure.

Wind Velocity Generation Method

Wind velocity field with longitudinal ($u_p(t)$), lateral ($v_p(t)$) and vertical ($w_p(t)$) components at spatial points P_i, is represented by the vector

$$\underline{u}_p(t) = \underline{\overline{u}}_p + \underline{u}'_p(t) \quad (6)$$

where $\underline{\overline{u}}_p$ is the vector of mean wind velocities composed of three components ($\overline{u}_p$, $\overline{v}_p$ and $\overline{w}_p$) and $\underline{u}'_p(t)$ is the fluctuating part. For spatially correlated wind velocities the Shinozuka–Deodatis method [6] is used

$$\underline{u}'_p(t) = \sqrt{\Delta\omega}\sum_{p}^{K}\sum_{j=1}^{N} T_{K,p}(\omega_{p,j})\cos(\omega_{p,j}t + \varphi_{p,j}) \quad (7)$$

where $\underline{u}'_p$ is the vector of fluctuating wind velocity which includes u'_p, v'_p and w'_p components in longitudinal, lateral and vertical wind directions. $\omega_{p,j}$ is frequency and $\varphi_{p,j}$ is random phase. $T_{K,p}(\omega_{p,j})$ are the elements of decomposed power spectral density (PSD) matrix $S_{\underline{u}'\underline{u}'}(\omega)$

$$\boldsymbol{S}_{\underline{u}'\underline{u}'}(\omega) = \begin{bmatrix} S_{\underline{u}'^{(1)}\underline{u}'^{(1)}}(\omega) & \cdots & S_{\underline{u}'^{(1)}\underline{u}'^{(K)}}(\omega) \\ \vdots & \ddots & \vdots \\ S_{\underline{u}'^{(K)}\underline{u}'^{(1)}}(\omega) & \cdots & S_{\underline{u}'^{(K)}\underline{u}'^{(K)}}(\omega) \end{bmatrix}. \quad (8)$$

The elements of the PSD matrix in equation (8) are cross-PSD functions computed from non-dimensional normalised PSD functions in the longitudinal, lateral and vertical direction, which were estimated in previous work [15]. The wind generation method was implemented in the developed WindSimul program.

Example

The above described computational scheme is demonstrated and was applied during the design stage in the example represented by a cable-stayed footbridge subjected to turbulent wind. The footbridge, situated in Kosice, Slovak Republic, (figure 1) has a span of 68m and the top of the pylon is at a height of 38.4m above the terrain. The pylon is inclined in the longitudinal axis of the footbridge with an angle of inclination of 9 degrees and the diameter of the cables is 72mm. A fan type cable system is applied for supporting the steel deck which comprises a closed cross-section stiffened with transversal plates every 2.5m.

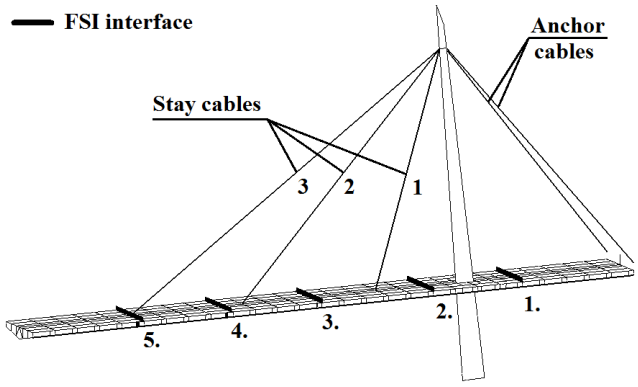

Figure 1. Geometry of footbridge and created five FSI Interfaces on the deck.

The CSD model consists of beam elements (cables) and shell elements (deck and pylon). The computed third eigenmode of the footbridge (first flexural eigenmode of the deck) with eigenfrequency $f_{0,3}$=2.359Hz using the modal analysis is shown in figure 2. The fourth eigenmode of the footbridge (second flexural eigenmode of the deck) corresponds to the eigenfrequency $f_{0,4}$=3.317Hz. The first torsional eigenmode of the deck corresponds to $f_{0,8}$=6.851Hz.

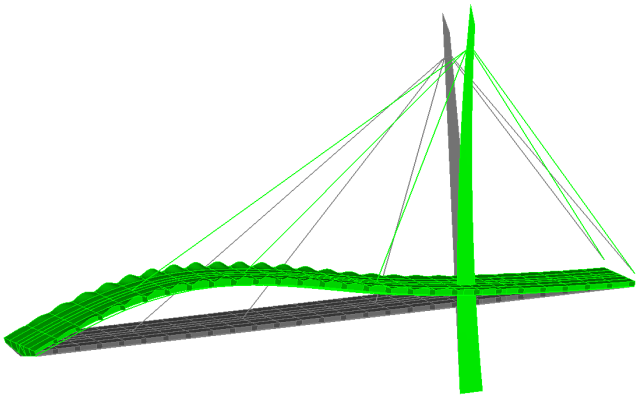

Figure 2. First flexural bending eigenmode of footbridge deck; black: initial geometry, green: computed eigenmode.

In order to solve turbulent flow the large-eddy simulation (LES) model is adopted. To assess preliminary parameters of the CFD model (mesh density and time step) the laminar fluid model was first applied. The LES model with a Smagorinsky constant of C_s=0.1 and time step Δt=0.001s is considered to be accurate enough after reaching the converged response (drag and lift forces, pitch moment and vortex shedding frequency f_{sh}=3.02Hz) and also the computational demands are acceptable. The CSD model is coupled with CFD model (figure 3) via FSI interface (figure 1, figure 4). The forces computed in CFD model can not be transferred to shell elements perpendicular to fluid planes. Therefore the beam coupling elements with the position identical to FSI interface, connected to the closest transversal deck stiffener via rigid links, are used.

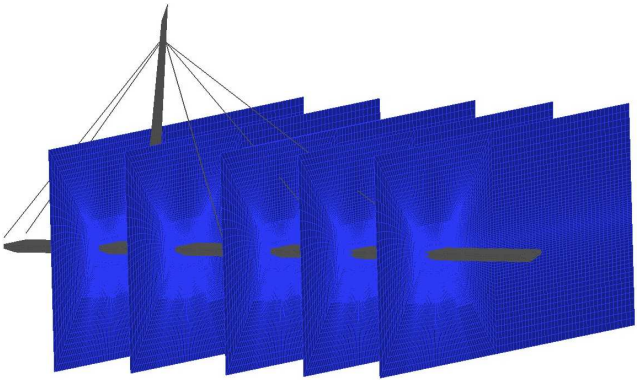

Figure 3. Coupled 3D CSD with 2D CFD.

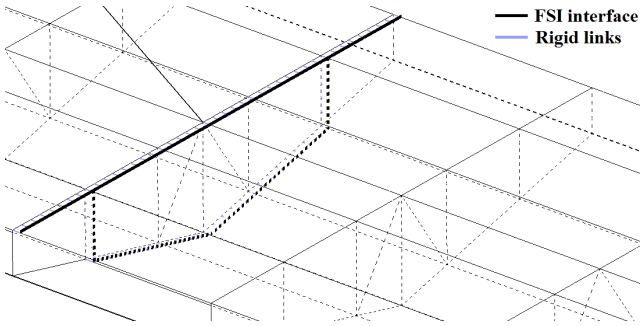

Figure 4. Detail view of FSI interface linked to transversal plate of the deck.

Spatially correlated wind velocities (in the longitudinal direction shown in figure 7) are generated at 32 points (figure 5), of which P1-P5 are located on the deck, P6-P11 and P32 are on the pylon and P12-P31 are on the cables. Figure 6 depicts the wind velocity

directions (longitudinal, lateral and vertical) applied in the wind velocity generation process which is a 3-dimensional 1-variate in this example. The mean wind velocity at deck level is 20m/s.

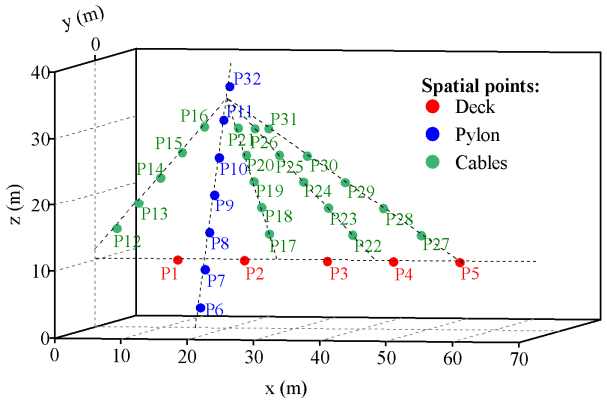

Figure 5. Spatial location of points for wind velocity generation.

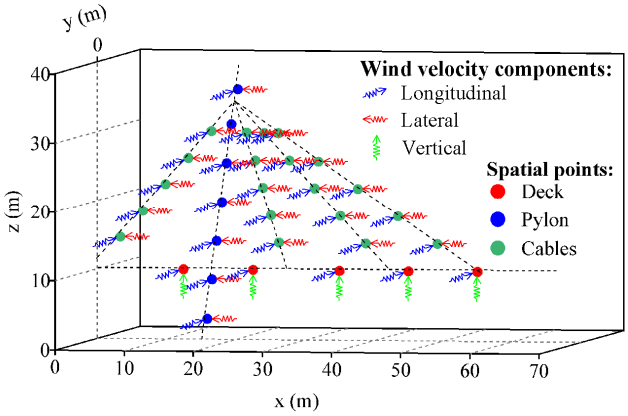

Figure 6. Components of generated wind velocities.

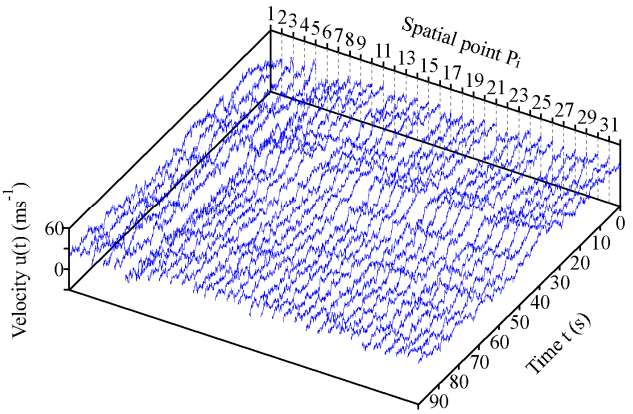

Figure 7. Generated wind velocities in longitudinal direction.

The aerodynamic forces acting on the cables and pylon in longitudinal and lateral direction are computed using

$$F_{y,p}(t) = \frac{1}{2}\rho A c_D \left(u_p(t)\right)^2, \quad (8)$$

$$F_{x,p}(t) = \frac{1}{2}\rho A c_L \left(v_p(t)\right)^2, \quad (9)$$

where A is the windward area, c_D and c_L denote the drag and lift coefficients of cables and pylon according to y and x coordinates. The aeroelastic forces acting on the deck are solved in the CFD model at each time step with applied wind velocity components $u_p(t)$ and $w_p(t)$ set up as the inflow parameter. The velocity component $v_p(t)$ acting on the deck is neglected in the simplified FSI method.

The computational procedure applied in the simplified FSI is divided into two computational stages (CS) as is shown in figure 8. In order to ensure the convergence between CSD and CFD models at the beginning of computations a large Rayleigh damping is applied in the 1.CS. After reaching the quasi-steady response of the deck the damping was reduced to 1% in the 2.CS.

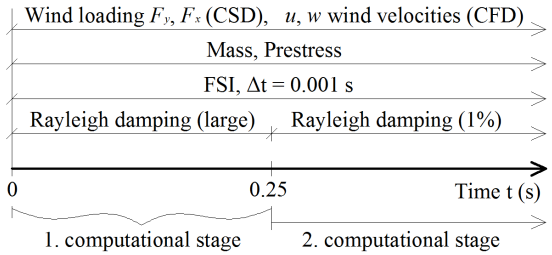

Figure 8. Simplified FSI computational procedure.

Response of Buffeting and VIVs in Interaction

The computed aeroelastic response of the footbridge in the time domain with a duration of 19.75s (time 0.25s-20s) is analysed. Time histories of vertical displacements of windward and leeward edges of the deck at the 3rd FSI interface are shown in figure 9. For both edges the vibration in the vertical direction occurs with frequencies of 2.4Hz and 3.2Hz as is shown in figure 10. These frequencies correspond to the first and second flexural eigenmode of the deck. There is almost a zero phase shift between the edges which denotes the torsional vibration mode is not excited. During the time from 13-18s the resonant flexural vibration mode of the deck has occurred.

In the previous analysis where a constant wind velocity of 20m/s was applied the vortex shedding frequency of f_{sh}=3.02 Hz was observed. Since the applied wind velocity has a turbulent nature, the f_{sh} might oscillate around this value. The result of this effect is apparent in figure 10, where the value of 3.2Hz is depicted.

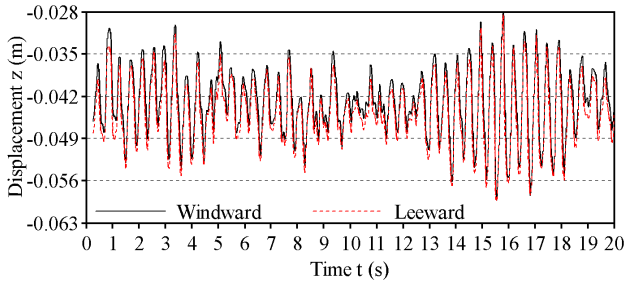

Figure 9. Vertical displacements of windward and leeward edges of the deck at 3rd FSI interface.

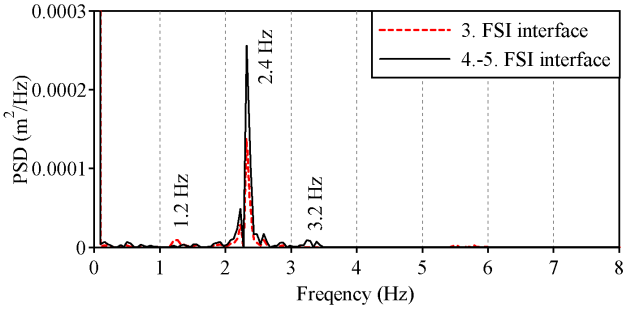

Figure 10. PSD of vertical displacements of the shear centre of the deck cross-section positioned at 3rd FSI interface and in the middle between 4th and 5th FSI interface.

The computed fluid flow around the footbridge deck at a time of 1.751s is shown in figures 11 and 12 located at the 3rd and 5th FSI interfaces, respectively. The shed vortexes leeward as well as the vortexes floating upward (figure 11) as a result of fluctuating wind with a strong vertical component can be recognized.

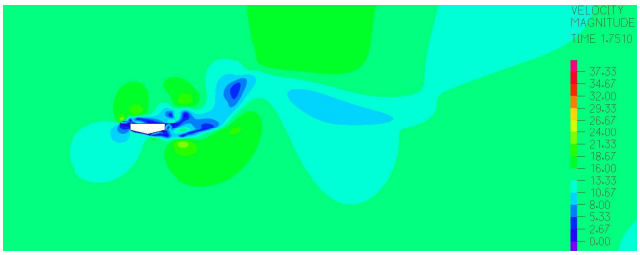

Figure 11. Velocity magnitudes around the deck at time 1.751s depicted at the 3rd FSI interface.

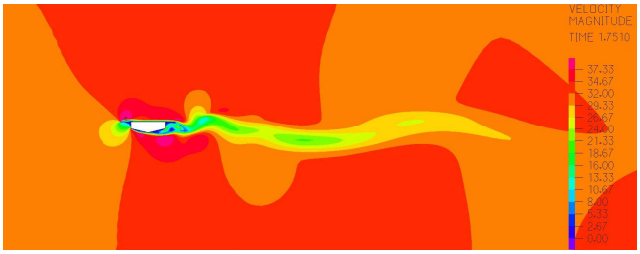

Figure 12. Velocity magnitudes around the deck at time 1.751s depicted at the 5th FSI interface.

Conclusions

The coupled CSD and CFD models via FSI interface with applied spatially correlated artificial wind velocity histories were applied to analyze the buffeting response interacting with VIVs of a cable-stayed footbridge.

The long-span structures are sensitive to turbulent wind forces producing a buffeting response which may result in fatigue damage. When considering the interaction of buffeting and VIVs this effect is more important.

The method can be applied to compute aeroelastic behaviour of long-span structures, such as bridges, with much less computational effort when compared to 3D CFD model around the entire length of deck. This method allows the inclusion of all the structural parts in the CSD model which leads to more accurate results.

Acknowledgments

This work is part of Research Project No. 1/0302/16, partially founded by the Scientific Grant Agency of the Ministry of Education of the Slovak Republic and the Slovak Academy of Sciences. This work was partially supported by the Slovak Research and Development Agency under the contract No. APVV-15-0777.

References

[1] Aas-Jakobsen, K. &Strømmen, E., Time Domain Buffeting Response Calculations of Slender Structures, *J. Wind Eng. Ind. Aerodyn.*, **89**, 2001, 341-364.

[2] ADINA, *Theory and modeling guide volume I: ADINA and volume III: ADINA CFD & FSI*, Version 8.7, ADINA R&D Inc, Watertown, MA, USA, 2010.

[3] Bruno, L. &Khris, S., The Validity of 2D Numerical Simulations of Vortical Structures Around a Bridge Deck, *Math. Comput. Model.*, **37**, 2003, 795-828.

[4] Caracoglia, L., Influence of Uncertainty in Selected Aerodynamic and Structural Parameters on the buffeting response of long-span bridges, *J. Wind Eng. Ind. Aerodyn.*, **96**, 2008, 327-344.

[5] Davenport, A.G., Buffeting of a Suspension Bridge by Storm Winds, *J. Struct. Div.*, ASCE, **88**(ST2), 1962, 233-268.

[6] Deodatis, G., Simulation of Ergodic Multivariate Stochastic Processes, *J. Eng. Mech.*, ASCE, **122**, 1996, 778-787.

[7] Ge, Y.T. &Xiang, H.F., Probability-based assessment of aerodynamic vibration of long-span bridges, in *Proceedings of the 9th International Conference on Structural Safety and Reliability*: ICOSSAR, 2005, 3856-3863.

[8] Hallak, P.H., Pfeil, M.S., de Oliveira, S.R.S., Battista, R.C., de Sampaio, P.A.B. &Bezerra, C.,M.N., Aerodynamic Behavior Analysis of Rio-Niterói Bridge by Means of Computational Fluid Dynamics, *Eng. Struct.*, **56**, 2013, 935-944.

[9] Hui, M.C.H., Larsen, A. &Xiang, H.F., Wind Turbulence Characteristics Study at the Stonecutters Bridge site: Part II: Wind Power Spectra, Integral Length Scales and Coherence, *J. Wind Eng. Ind. Aerodyn.*, **97**, 2009, 48-59.

[10] Jones, N.P. &Scanlan, R.H., Theory and Full-Bridge Modeling of Wind Response of Cable-Supported Bridges, *J. Bridge Eng.*, ASCE, **6**(6), 2001, 365-375.

[11] Löhner, R., Haug, E., Michalski, A., Muhammad, B., Drego, A., Nanjundaiah, R. &Zarfam, R., Recent Advances in Computational Wind Engineering and Fluid-Structure Interaction, *J. Wind Eng. Ind. Aerodyn.*, **144**, 2015, 14-23.

[12] Stoyanoff, S., A Unified Approach for 3D Stability and Time Domain Response Analysis with Application of Quasi-Steady Theory, *J. Wind Eng. Ind. Aerodyn.*, **89**, 2001, 1591-1606.

[13] Sun, D.K., Xu, Y.L. &Ko, J.M., Fully Coupled Buffeting Analysis of Long-Span Cable-Supported Bridges: Formulation, *J. Sound Vibration*, **228**(3),1999, 569-588.

[14] Soltys, R., Tomko, M. &Kmet, S., Analysis of Wind-Induced Vibrations of an Anchor Cable Using a Simplified Fluid-Structure Interaction Method, *Appl. Math. Comput.*, **267**, 2015, 223-236.

[15] Tomko, M., Kmet, S. &Soltys, R., Vibration of an Aramid Anchor Cable Subjected to Turbulent Wind, *Adv. Eng. Software*, **72**, 2014, 39-56.